Effect of reinforcement size and orientation on the thermal expansion behavior of metallic glass reinforced metal matrix composites produced by gas pressure infiltration

Klaudia Lichtenberg, Kay A. Weidenmann

Angaben zur Veröffentlichung / Publication details:

Lichtenberg, Klaudia, and Kay A. Weidenmann. 2017. "Effect of reinforcement size and orientation on the thermal expansion behavior of metallic glass reinforced metal matrix composites produced by gas pressure infiltration." *Thermochimica Acta* 654: 85–92. https://doi.org/10.1016/j.tca.2017.05.010.

Effect of reinforcement size and orientation on the thermal expansion behavior of metallic glass reinforced metal matrix composites produced by gas pressure infiltration

Klaudia Lichtenberg*, Kay André Weidenmann

Karlsruhe Institute of Technology (KIT), Institute for Applied Materials (IAM-WK), Engelbert-Arnold-Str. 4, 76131 Karlsruhe, Germany

1. Introduction

Metal matrix composites (MMCs) offer the advantage of adaptability of desired material properties for specific applications. Therefore, they are applied e.g. in electronic applications instead of single alloys when high thermal conductivity and low thermal expansion are required [1,2]. Although MMCs offer better high temperature properties than the unreinforced alloy, they show a complex behavior when heated due to different thermal and mechanical properties of the single components [3], like Young's moduli and thermal expansion coefficients (CTE). Materials normally used as reinforcements, like ceramics, usually exhibit higher Young's moduli and lower coefficients of thermal expansion (CTE) than the commonly used matrix materials. This leads to formation of internal stresses due to the mismatch in thermal expansion and elastic properties of the components. The lower CTE of the reinforcement phase further causes a reduced thermal expansion of the composite [4] as desired for electronic applications. Further, the thermal behavior of composites also depends on reinforcement volume fraction, the arrangement of the reinforcement within the composite and on defects, like microscopic pores or cracks, originating during composite processing [5]. As an example: Particle reinforced MMCs exhibit nearly isotropic behavior with lower CTEs than the unreinforced matrix [6], while MMCs with fibrous reinforcements show accumulated macroscopic plastic deformation [7] with significant anisotropy depending on fiber orientation [8–11]. Hence, comprehensive investigations on understanding the numerous influencing factors on the thermal expansion behavior of different composites are essential for an extension of the application range.

Investigations on the thermal expansion behavior of composites based on AlSi-alloys with reinforcement of SiC-particles and various reinforcement volume contents were performed by Ref. [6]. They revealed that the thermal expansion of composites with isolated particles can be described by the thermal expansion behavior of the AlSi-matrix [6]. The CTE(T)-curve of these composites exhibits the same shape as for the single AlSi-alloy with the same decrease in CTE at high temperatures due to increasing solubility of silicon in aluminum with increasing temperature [12]. The increase of reinforcement volume fraction just leads to lower levels of CTE-values [6,13]. Their investigations on a composite consisting of an infiltrated SiC sintered preform further showed that the composite's CTE at high temperatures

* Corresponding author.
E-mail address: Klaudia.Lichtenberg@kit.edu (K. Lichtenberg).

matches the CTE of bulk SiC due to the rigidity of the preform [6].

Over the last years, several studies dealt with the mechanical properties of MMCs with metallic glass reinforcements and showed their high potential concerning enhanced Young's modulus and strength [14–18]. To date no investigations were performed on the thermal properties of these composites although the difference in thermal expansion coefficients and correlated internal stresses are also present in MMCs reinforced with metallic glass. Therefore, it is inevitable to characterize their thermal properties in detail to obtain a comprehensive view on materials processing-structure-property-relations to develop new areas of application. In this study, the thermal expansion behavior of several metallic glass flake reinforced composites with different size ranges produced by gas pressure infiltration is investigated. Thermal expansion characterization is carried out with a special focus on the influence of flake size and flake orientation. The composites will be examined by means of dilatometry during four thermal cycles between room temperature and 500 °C. CTEs determined by these measurements will be further compared with several thermo-mechanical models.

2. Experimental procedure

2.1. Material

As matrix material, the unrefined aluminum alloy AlSi12 (EN AC-44200) was utilized. Metallic glass $Ni_{60}Nb_{20}Ta_{20}$ with a crystallization temperature of T_x = 723 °C [19] was used as reinforcement in the studied composites. The metallic glass was produced by Fraunhofer Institute IFAM (Dresden, Germany) as melt spun ribbons with a mean thickness of 50 µm. The reinforcement flakes were prepared by ball milling these ribbons. The milled ribbons were sieved to separate different flake size ranges. The different size ranges are listed in Table 1.

The composites investigated in this study were fabricated by conventional gas pressure infiltration of the respective flake size and aspect ratio ranges (cf. Table 1). At the beginning of the infiltration process, the processing chamber was evacuated to 0.08 mbar and purged with argon to remove remaining oxygen. The processing chamber was heated with constant heating rate of 5.5 °C/min to the maximum processing temperature of 660 °C. This maximum temperature was held for 2 h during the melting of the matrix raw material and homogenization of the melt. Infiltration was achieved by argon with a pressure of 40 bar. This pressure was held during cooling down the processing chamber with constant cooling rate of 5.5 K/min. Previous investigations including X-ray diffraction measurements proved that it is possible to produce composites using these processing parameters without crystallization of the metallic glass since the maximum processing temperature is lower than its crystallization temperature [15]. For a detailed processing technique description, processing parameters and infiltration device, we refer to Refs. [15] and [18].

Investigated flake size ranges and aspect ratios, measured density and calculated average volume content of reinforcements within the composite are given in Table 1. Since smaller particles lead to smaller inter-particle distances [20], increasing volume fractions of metallic glass within the composites can be realized with decreasing flake sizes.

Table 1
Flake size and aspect ratio ranges used in this study and resulting average composite density and reinforcement volume fraction.

Composite	Flake size range (µm)	Flake aspect ratio	Density (g/cm^3)	Reinforcement volume fraction (%)
A	100–200	2–4	6.03 ± 0.07	43.1 ± 0.9
B	200–600	4–12	5.59 ± 0.13	37.6 ± 1.7
C	600–2000	12–40	4.93 ± 0.09	29.1 ± 0.9

It is not possible to adjust reinforcement volume fractions to a defined level due to processing restrictions.

2.2. Structural analysis via X-ray micro computed tomography (µCT)

As shown in [15] for large flake sizes, metallic glass flakes within the composites are supposed to be oriented perpendicular to the infiltration direction of the melt into the mold during processing due to the plate-like shape of the flakes and the high aspect ratios. To prove this assumption for the composites of this study, 3D X-ray micro computed tomography (µCT) investigations were carried out on selected samples. For this purpose, an Yxlon Precision computer tomograph with a flat panel detector from Perkin Elmer and a tungsten target were used. Acceleration voltage was fixed to 180 kV and the target current was 0.02 mA. The scan consisted of 2400 projections during a 360° sample rotation along the vertical axis with an integration time of 700 ms per projection. Scan resolution was 4.31 µm/voxel. The image data was rendered using the image processing program Avizo.

Orientation of the flakes was analyzed using the aligned and cropped µCT data. Therefore, orientation of the normal vector in each voxel (c.f. Fig. 4(a)) was calculated using a method based on the structure tensor [21]. This method was earlier implemented in the open source project *Composight* [22] for fibrous materials [23] and was modified for application with planar structures. The algorithm is mostly equal to that for fibers, but the direction of a normal vector of a plane is given by the largest eigenvalue of the structure tensor and its corresponding eigenvector instead of the lowest eigenvalue as for fibers. Results of this orientation analysis are given as orientation histograms showing the number of voxels in a µCT image with an absolute deviation angle from a defined axis.

2.3. Dilatometer measurements

Investigations on the thermal expansion behavior of the metallic glass reinforced composites were carried out in a common push-rod dilatometer type DIL 805A/D from Bähr-Thermoanalyse GmbH (Hüllhorst, Germany). The device consists of a fixed push-rod and a variable rod which is connected to a linear variable differential transformer (LVDT) for measuring sample dilatation. Heating is realized by an induction coil. A separate perforated coil for gas quenching is used in parallel. Further information about the dilatometer setup are given in Ref. [24]. In this investigation, parallelepiped samples of each composite with dimensions of 7 × 4 x 4 mm^3 were taken from the infiltrated material by electrical discharge machining. Matrix material samples with the same temperature history as the composites were taken as reference. Edges of the samples were deburred to ensure adequate contact of the sample with the push-rods inside the dilatometer. Since processing restrictions and flake aspect ratios are expected to lead to a layered flake arrangement within the composite with flake orientation perpendicular to the infiltration direction (see Sections 2.2 and 3.1), samples were taken from the infiltrated material with different orientations concerning the infiltration direction. Fig. 1 illustrates the layered reinforcement structure within the composite including exemplary samples and testing directions. As depicted, samples were studied in longitudinal direction along flake orientation (along y-axis) and in transverse direction perpendicular to flake orientation (along z-axis).

The temperature-dependent elongation of the samples was measured along the major axis of each sample (see Fig. 1). Four thermal cycles between room temperature and 500 °C with constant heating and cooling rate of 5 °C/min were recorded for each sample. The thermal expansion was measured during heating and cooling. The experiments were performed in an inert helium atmosphere to avoid oxidation of the composites. All experimental data was corrected by a reference measurement with a platinum sample to eliminate any thermal length change effects of the testing device as required by Ref. [25].

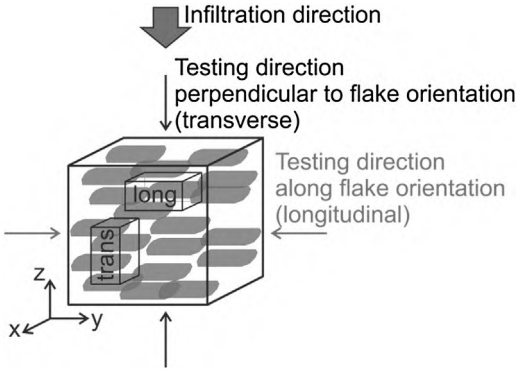

Fig. 1. Schematic of the layered reinforcement arrangement within the composite including exemplary samples and testing directions with respect to flake arrangement (along and perpendicular to flake orientation).

The temperature-dependent thermal strain during heating and cooling was calculated using the measured length change of the sample and the length of the sample L_0 at the beginning of the measurement. Due to non-equidistant experimental data, determination of the temperature-dependent coefficient of thermal expansion (CTE) by derivation of the calculated thermal strain was not directly possible. Therefore, thermal strain data was first approximated by a sixth-order polynomial (R-Square (COD) = 1) in each heating and cooling section to obtain a continuously differentiable function. CTE was subsequently determined by differentiation of the polynomial fit.

3. Results

3.1. Micro computed tomography (μCT)

Visualized 3D-results of the μCT scans on selected dilatometer samples of all investigated composite types are shown in Figs. 2 and 3. The figures show that the plate-like shaped flakes in composite B and C with large flake sizes are oriented perpendicular to the infiltration direction (z-axis) during processing as was expected from Refs. [15] and [18]. The layered flake arrangement is attributed to compacting effects during mold filling and processing enhanced by the plate-like shape and the high aspect ratio of the flakes. μCT scans of the composite A samples reveal only slight differences in flake orientation due to a smaller aspect ratio of the flakes.

Results of the orientation analysis performed on the μCT data shown in Fig. 3 are displayed in Fig. 4(b). The results are given as a distribution of the number of voxels as a function of the absolute deviation angle θ between normal vector $\vec{n}$ and z-axis which is parallel to the infiltration direction (c.f. Fig. 4(a)). All distribution data was normalized by the total number of voxels. It is shown that composite C with largest flake sizes exhibits the narrowest distribution of flake orientation perpendicular to infiltration direction. Preferred orientation is less distinct with larger angular deviation for composites B and A with smaller flake sizes due to the smaller aspect ratios compared to composite C (see Table 1). It was determined from the distribution function that 50 % of the counted voxels for composite A exhibit a maximum deviation angle $\theta_{50\%}$ of 41°. For composite B, maximum deviation angle $\theta_{50\%}$ is 20° and for composite C $\theta_{50\%}$ is only 14°.

3.2. Thermal expansion behavior

Fig. 5 illustrates the temperature-dependent evolution of the thermal strain during the four thermal cycles of the AlSi-reference (a) and of composite B (b) tested along (longitudinal) and perpendicular (transverse) to the flake orientation, which shows representative behavior for all composites. The samples exhibit thermal hysteresis with highest extent during the first cycle. For cycles 2, 3 and 4, thermal hysteresis are minimal and no further significant changes occur. The samples show some remaining negative thermal strain after the four cycles.

As internal stresses are generated in metal matrix composites during solidification, the thermal history must be considered during investigation of the composites' thermal behavior [6]. A high extend of thermal hysteresis during the first cycle indicates that processing history influences thermal expansion behavior. As following cycles show nearly identical behavior, stress state and microstructure in the sample have stabilized as slow heating and cooling rate allow for creating a thermodynamic equilibrium [6,26]. To exclude these prior processing influences, thermal properties of the composites will be further studied for the second heating, when eventual material instabilities are annealed and material's behavior is more representative.

Fig. 6 shows the evolution of thermal strain of the tested samples during the second heating. It is observed that metallic glass volume content, flake size and flake orientation seem to have a strong influence on the composite's behavior. All composite samples exhibit higher transverse than longitudinal thermal strains. For composite B and C, transverse thermal strain perpendicular to flake orientation is even higher than for the matrix reference. While the matrix reference sample exhibits a maximum of thermal strain of 1.13% at maximum temperature, transverse thermal strain for composite B and composite C tested perpendicular to flake orientation (cf. Fig. 3) accumulates up to 1.21% and 1.55% respectively. For testing direction along flake orientation

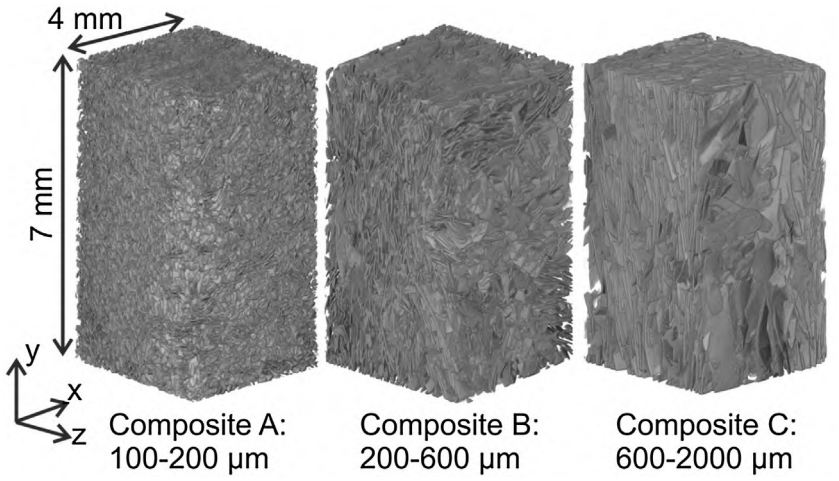

Fig. 2. Rendered 3D-models of the metallic glass arrangement within the dilatometer samples with flake orientation along testing direction (longitudinal) of composite A, B and C obtained by micro computed tomography (μCT).

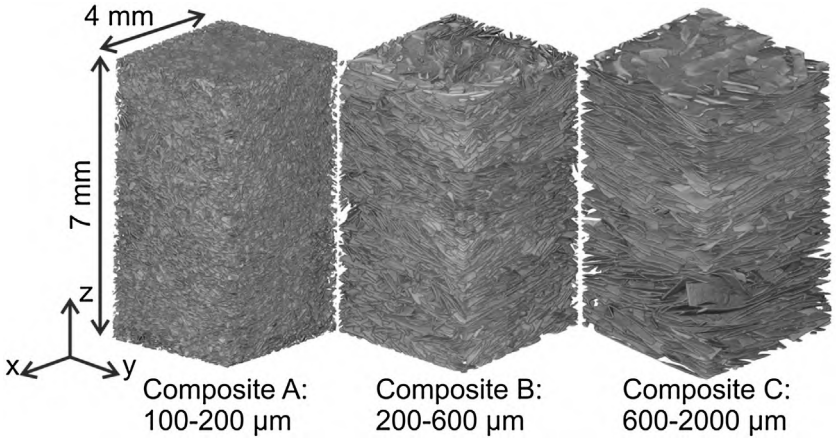

Fig. 3. Rendered 3D-models of the metallic glass structure within the dilatometer samples with flake orientation perpendicular to testing direction (transverse) of composite A, B and C obtained by micro computed tomography (µCT).

(longitudinal), these composites show the lowest overall thermal strain. All composite samples, regardless of testing direction, display a change in slope of the thermal strain-temperature curves at about 200 °C.

Coefficients of thermal expansion of the composites as well as the matrix material are not linear with increasing temperature and the composites exhibit a distinct anisotropy depending on flake orientation. This behavior is shown in Fig. 7 for all studied samples for the second heating cycle. It is observed that the CTE(T)-curves show a similar trend as the thermal strain curves displayed in Fig. 6.

The determined CTE of the AlSi-matrix is 20×10^{-6}/K at room temperature and increases to a maximum of 26×10^{-6}/K at approx. 400 °C. At higher temperatures, the CTE of the AlSi-matrix sample decreases. Similar behavior is observed for composites B and C tested perpendicular to flake orientation (transverse) and for composite A for both testing directions. But while composite A shows an overall increase in CTE for both testing directions, composites B and C exhibit distinct increase in CTE when tested perpendicular to flake orientation (transverse) and slight decrease in CTE when tested along flake orientation (longitudinal). For testing direction along flake orientation, longitudinal CTE of composite A shows a slight increase from 14×10^{-6}/K at room temperature to 15×10^{-6}/K at 400 °C and a slight decrease afterwards following the same shape as the AlSi-reference. By contrast, longitudinal CTE of composite B decreases from 14×10^{-6}/K to 13×10^{-6}/K at 200 °C and remains nearly constant. Longitudinal CTE of composite C follows the same trend by decreasing from 15×10^{-6}/K to 12×10^{-6}/K at 200 °C remaining nearly constant afterwards, too. When tested perpendicular to flake orientation, transverse CTE of composite A increases from 15×10^{-6}/K at room temperature to 24×10^{-6}/K at 400 °C, transverse CTE of composite B rises from 15×10^{-6}/K to 31×10^{-6}/K and transverse CTE of composite C from 17×10^{-6}/K to even 41×10^{-6}/K. CTE of all these samples shows a slight change in slope at approx. 100 °C and distinct decrease after reaching their maximum at approx. 400 °C.

4. Discussion

The CTE of metal matrix composites is generally temperature-dependent due to influences of prior stress history caused by processing, reinforcement volume fraction and reinforcement architecture as well as the presence of defects like microscopic pores or cracks [3]. The metallic glass reinforced composites examined in this study show that the thermal expansion behavior seems to strongly depend on the behavior of the constituent phases and the mentioned layered flake arrangement within the composite. Detailed effects on this behavior will now be further discussed.

All composites containing components with strongly differing coefficients of thermal expansion exhibit residual thermal stresses after processing. These residual thermal stresses are generally expected to be tensile within the matrix and compressive within the reinforcement, when the CTE of the matrix material is higher than the CTE of the

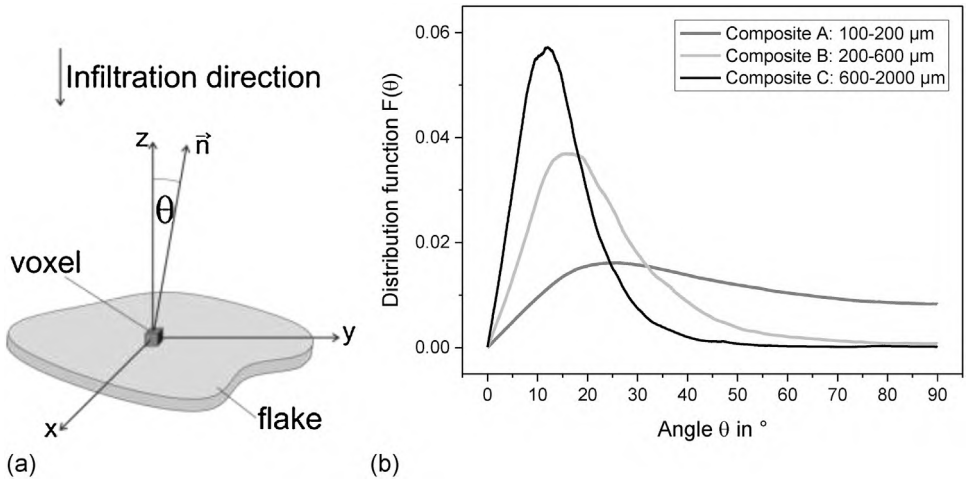

Fig. 4. Schematic depiction of one exemplary voxel within a flake and its normal vector $\vec{n}$ and deviation angle θ from z- axis (a) and results of the orientation analysis performed by the described method on the µCT data; the results are given as distribution function (normalized by the total number of voxels) showing the number of voxels in a µCT image as a function of the absolute deviation angle θ (b).

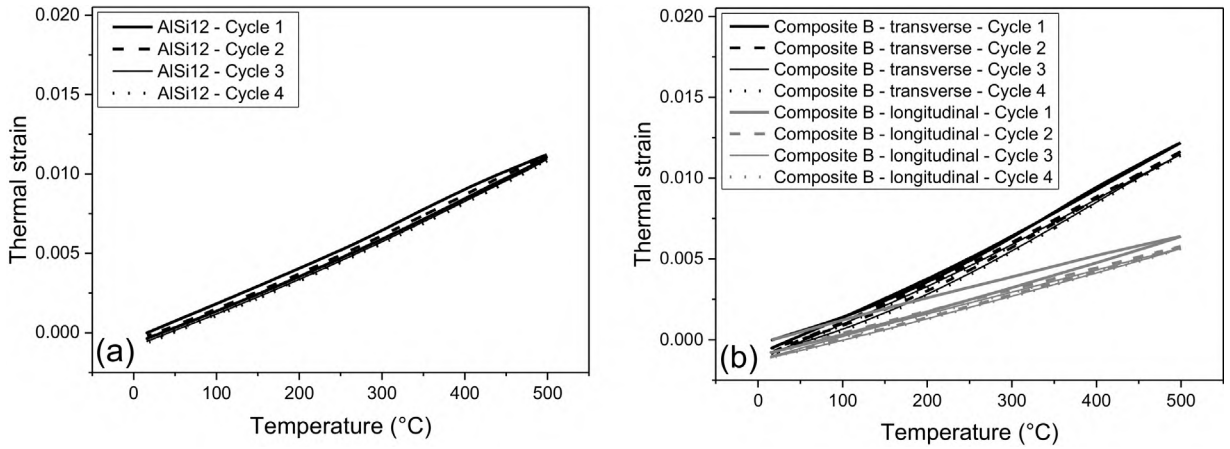

Fig. 5. Evolution of thermal strain during the four thermal cycles for the AlSi12 reference (a) and composite B (b) tested along (longitudinal) and perpendicular (transverse) to the flake orientation.

reinforcement phase [26,27]. With increasing temperatures, new thermal stresses will develop in both phases [26]. The yield stress of the matrix phase further decreases with increasing temperature and the combination of these effects will lead to initiation of plastic deformation at a certain temperature. Due to the thermal behavior of the composites in this study with change in slope of the CTE(T)-curves of the composites (c.f. Fig. 7), it is expected that plastic deformation starts within the temperature range of 100–200 °C. Similar observations and conclusions were drawn in [1,12,26]. The effect gets even more obvious at 200 °C by the change in slope of thermal strain evolution (c.f. Fig. 6). From this temperature, all studied composites exhibit an anisotropic behavior with higher thermal strains and coefficients of thermal expansion in transverse direction perpendicular to flake orientation than in longitudinal direction. Most distinctive effects with highly anisotropic behavior are observable for composite C with the largest flake size and tight orientation of the flakes perpendicular to infiltration direction (c.f. Fig. 4(b)).

Measurement of the CTE of the metallic glass was not possible due to the small sizes of the metallic glass ribbons. Further, no CTE values of the metallic glass $Ni_{60}Nb_{20}Ta_{20}$ are available in literature data due to the large variety of glass-forming alloys. However, empirical studies on various metallic glasses in Ref. [28] revealed a relation between glass temperature and CTE. It was shown that the product of CTE and glass temperature $\alpha_g \cdot T_g$ that matches approximately to the value 8.4×10^{-3} for the linear α_g-range up to 100–50 K below T_g [28]. Therefore, CTE of the metallic glass used in this study was estimated using this relation. It was further assumed that the metallic glass $Ni_{60}Nb_{20}Ta_{20}$ exhibits a linear thermal expansion below the glass transition temperature as shown for other metallic glasses [28,29]. Due to a lack of literature data, the CTE of the metallic glass $Ni_{60}Nb_{20}Ta_{20}$ was estimated to approx. 9.0×10^{-6}/K by using data of the metallic glass $Ni_{60}Nb_{30}Ta_{10}$ with similar chemical composition (T_g = 934 K [19]). Hence, CTE of the metallic glass is assumed to be significantly lower than the CTE of the AlSi-matrix (see Fig. 7). Further supposing isotropic thermal expansion behavior of the metallic glass, the anisotropic behavior of the composites can be explained using the schematic depiction in Fig. 8. Fig. 8(a) shows a schematic volume element of the matrix which expands isotropic with increasing temperature in the unreinforced state. In comparison, Fig. 8(b) schematically depicts a comparable volume element of the composite. Within the composite, thermal expansion of the matrix is hindered due to the lower CTE of the metallic glass compared to the matrix. This is caused by local equal-strain condition due to good interfacial bonding which is known to exist within metallic glass reinforced metal matrix composites [17]. To fulfill the constant volume condition on the other hand, this constraint of the matrix needs to be compensated by extensive thermal expansion perpendicular to the flakes. Therefore, the measured thermal expansion and CTEs are significantly lower in longitudinal direction along flake orientation than perpendicular to it in transverse direction. Transverse thermal expansion behavior of the composite is therefore controlled by the matrix material which is expected to soften with increasing temperature and to deform plastically. Along flake orientation, thermal expansion behavior of the composite is controlled by the metallic glass reinforcement which hinders thermal expansion of the matrix. Similar effects showing enhanced anisotropy with higher thermal expansion and CTE perpendicular to the fiber plane than parallel to it were

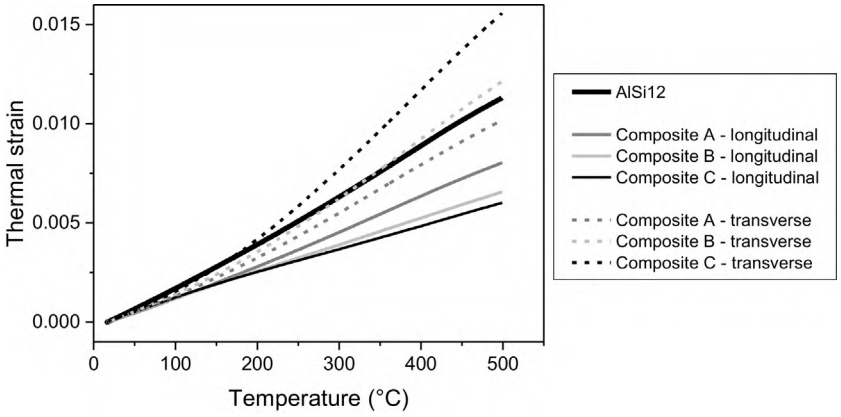

Fig. 6. Evolution of thermal strain during the second heating for the different composites with various metallic glass volume content and different flake orientations in comparison to the unreinforced matrix sample as reference.

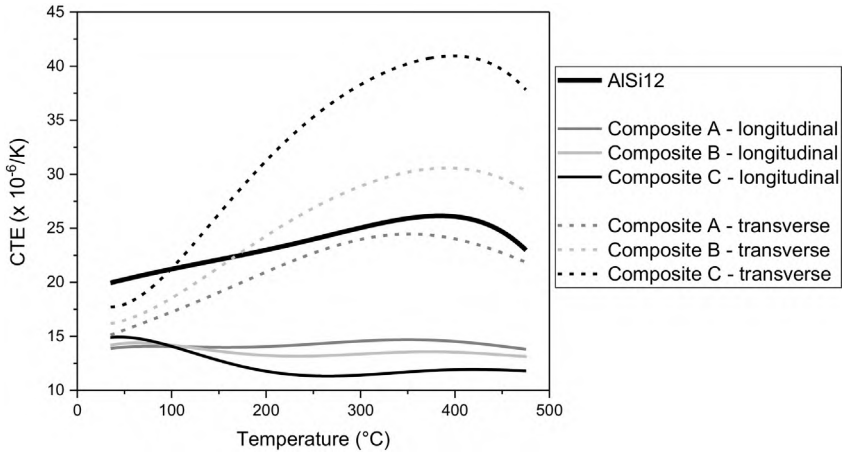

Fig. 7. Evolution of the coefficients of thermal expansion (CTE) during the second heating for the different composites with various metallic glass volume content and different flake orientations in comparison to the matrix material sample as reference.

observed for ceramic reinforced composites with long fiber [10,11] and short fiber reinforcement [8,9] as well as for composites reinforced with lamellae ceramic structures produced by freeze casting [26].

In case of strong constraint of thermal expansion of the matrix as it is known from composites with interpenetrating ceramics, the CTE of the composite approaches the CTE of the reinforcement [6]. In case of composite C with the largest particle sizes and distinct orientation, constraining effects on the matrix seem to be most effective due to the measured pronounced anisotropy. Therefore, CTE values of the composite are expected to approach the assumed CTE of the metallic glass with increasing temperatures reaching a value of 11–12 $\times$ 10^{-6}/K for the composite which is close to the estimated CTE value of the metallic glass.

However, a similar trend as for composite C is shown for composite B. But as flakes are smaller than in composite B and flake orientation is less pronounced (c.f. Fig. 4(b)), the thermal expansion constraint on the matrix along flake orientation is expected to be lower leading to less intense anisotropy. For composite A with the smallest flake sizes, the anisotropy is even less showing a lower CTE than the unreinforced matrix material and CTE(T)-curves following the same shape as the matrix. This suggests that the CTE of the composite A is completely controlled by matrix material behavior, with lower CTE than the matrix due to the presence of the reinforcement phase [6,26]. Therefore, thermal expansion mechanisms seem to change from short fiber reinforcement-like behavior as it was observed in Ref. [9] to particle reinforcement-like behavior [6]. Decreasing thermal strain with increasing reinforcement volume fraction as shown for particle reinforced composites [13] was generally not observed in this study. But since shape and 3D arrangement of the flakes have a great influence on the thermal expansion behavior of the composites, no conclusions can be drawn concerning the influence of reinforcement volume content in this contribution and further experiments using similar flake sizes with different reinforcement volume fractions need to be carried out.

The decrease in CTE of the AlSi-matrix as observed at high temperatures can be attributed to partial re-dissolution of Si starting at high temperatures (at about 300 °C) as solubility of Si in the Al-lattice increases with increasing temperature (250 °C: 0.05 wt%; 500 °C: 0.8 wt%) [6,12,30]. This partial re-dissolution leads to a further decrease of the CTE due to the reduced atomic volume of the substitutional Si-atoms within the Al-lattice [6,12,31]. During cooling, re-dissoluted Si precipitates again starting at about 400 °C [6]. This process is completely reversible as long as slow heating and cooling rates are employed which allow for establishing a thermodynamic equilibrium [6]. As this behavior is typical for Al-Si alloys [12] and was extensively discussed before [6,12], it will not be discussed in detail in this contribution. Similar behavior as for the unreinforced matrix material is observed for composites B and C tested perpendicular to flake orientation (transverse) and for composite A for both testing

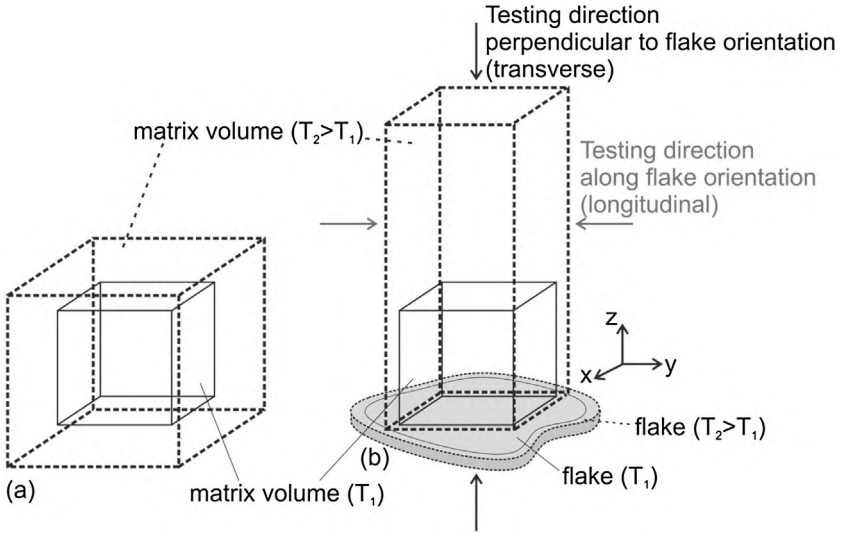

Fig. 8. Schematic of the isotropic thermal expansion behavior of the unreinforced matrix (a) and the anisotropic behavior of the composite (b) caused by constraint of thermal strain of the matrix along flake orientation due to the reinforcement and thermal strain compensation perpendicular to flake orientation due to constant volume condition.

directions. It is expected that similar reversible re-dissolution and precipitation effects as in the matrix material occur within the composites due to the slow heating and cooling rates which were used in this study.

Coefficients of thermal expansion of metal matrix composites are difficult to predict by thermo-mechanical models because there are many influencing factors [3,13]. To exclude any influence of measurement effects during the first cycle because of thermal history due to processing or because of microstructural changes, CTE of the second heating was taken to calculate the CTEs of the composites. The Schapery model [32], Turner model [33], Kerner model [34] and Wakashima model [35] were calculated to determine the coefficients of thermal expansion. While the Kerner model assumes spherical particles and a uniform wetting layer of matrix [13,34], it coincides with Schapery upper bound [32]. The Schapery upper bound describes CTEs of composites with isolated particle structure and Schapery lower bound CTEs of MMCs with 3D penetrating structures [6]. The Turner model assumes continuous reinforcements with equal-strain condition and neglects shear deformation [13]. In contrast, the Wakashima model gives values for disc-shaped particles (i.e. flakes) along (longitudinal) and perpendicular (transverse) to the particle alignment [35]. As input variables, the measured CTE of AlSi12 and the estimated CTE-value of the metallic glass (due to Ref. [28]) have been used for calculations of the models.

These listed models are only valid as long as there is elastic deformation within the composite [1]. Therefore, CTEs of the composites were calculated for the temperature range 20–100 °C where no plastic deformation is expected due to the results of this study. Temperature-dependence of Young's modulus, shear and bulk modulus was neglected. It is expected that deviations of experimental data is larger than the influence of temperature change in Young's modulus anyways. Further, there is no significant change in thermal hysteresis (cf. Fig. 5) and therefore no significant thermal damage or change in properties like degradation of the glass occurs. Thus, possible influences of thermal cycling on the properties of the metallic glass like structural relaxation are disregarded for the calculations. Results of the calculations in comparison to experimental results are shown in Fig. 9.

Fig. 9 shows that all composite CTEs lie in between the bounds given by Turner model and Wakashima upper bound (transverse). With smaller flake sizes, CTEs seem to approach a more isotropic behavior which is described by the Kerner model. This might be concluded as longitudinal CTE of composite A with small flake sizes and high level of flake misalignment lying in between both Schapery bounds close to the Kerner model. On the contrary, larger flake sizes associated with a higher level of flake alignment due to decreasing deviation angle θ lead to higher anisotropic thermal expansion behavior with increasing distance between longitudinal and transverse thermal expansion. This is particularly shown for composite C: Here, the Wakashima lower bound seems to give adequate estimation of the longitudinal thermal expansion behavior of composite C, while transverse CTE of composite C matches Wakashima upper bound. The Wakashima lower bound also gives a good approximation of the longitudinal thermal expansion behavior of composite B. Transverse CTE of composites A and B are not described by any model.

The obtained results imply that the Wakashima model for disc-shaped particles gives a good estimation for the composite C with large plate-like flakes and a high level of flake alignment within the composite. Composite A with smallest flake sizes and high flake misalignment can be treated as particle reinforced-like behaving composite and longitudinal CTE might be approximated by Kerner model. Composite B with large flakes and decreasing flake orientation cannot be described by the listed thermo-elastic models properly since its behavior features CTE-characteristics of both disc-shaped flakes and particle-like reinforcement. Further, it is not possible to give reliable estimation for the CTE in transverse direction for these composites with smaller flake sizes and higher misalignment since thermal expansion mechanisms seem to be more complex.

Although there is a good estimation for the longitudinal CTEs of the studied composites and the composite with large flake sizes and alignment, applicability of these simple models is limited since many assumptions were made for idealized conditions concerning reinforcement arrangement, load transfer and deformation behavior. Influences by complicated reinforcement shapes, microscopic pores or premature microplasticity at sharp reinforcement edges due to mismatch in CTE of the components lead to further inaccuracies and uncertainties. Therefore, the results need to be validated by further experiments and detailed FE-simulations should be carried out to reach a higher reliability of the results.

5. Conclusions

In this study, investigations on the thermal expansion behavior of metallic glass flake reinforced metal matrix composites were carried out considering the dependence on flake size and orientation. Several composites with different flake sizes and volume fractions were prepared by gas pressure infiltration. The 3D arrangement of the metallic glass flakes within the composites was investigated by means of micro computed tomography (μCT). Thermal expansion behavior was then studied by dilatometry measurements. Therefore, the following main conclusions can be drawn:

- The composites exhibit an aligned flake structure perpendicular to infiltration direction with increasing deviation angle, i.e. increasing misalignment with decreasing flake size and aspect ratio.
- The composites show significant thermal anisotropy due to flake orientation. This anisotropy is more distinct with larger flakes.

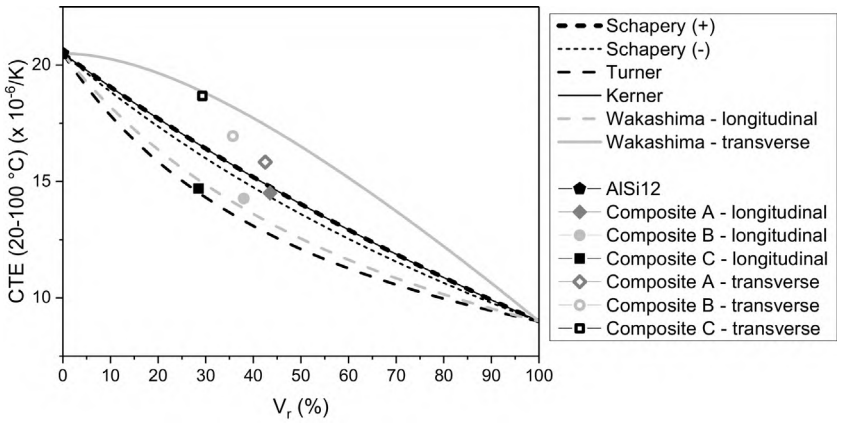

Fig. 9. Measured CTEs of the various composites tested along and perpendicular to the flake orientation in comparison with several thermo-elastic models.

- Size and 3D-arrangement of the flakes seem to have greater influence on the thermal expansion behavior of the composite than reinforcement volume fraction. But due to current processing restrictions, detailed study on the influence of reinforcement volume fraction with constant flake size and orientation was not possible by now and further experiments need to be carried out to draw further conclusions.
- No changes in thermal hysteresis is observed during thermal cycling, therefore no distinct thermal damage is expected.
- The Wakashima model seems to give a good estimation for both longitudinal and transverse CTE of the composites with large flakes sizes and a high level of flake alignment due to small deviation angles. Composites with small flake sizes and increasing flake misalignment are likely to approach Kerner model. However, it was not possible to give reliable estimation for CTE in transverse direction for the composites with increasing flake misalignment.

Although flake orientation allows for tailoring desired thermal properties, application possibilities, e.g. in electronic applications, of anisotropic materials are mostly limited due to potential mismatch between components. Thus, composites with smaller metallic glass flake size fractions, which are expected to behave isotropic, will be studied in further investigations.

Acknowledgements

The authors are thankful to Fraunhofer Institute IFAM (Dresden, Germany) for producing the metallic glass ribbons. Further, the authors would like to thank Sergej Ilinzeer for processing µCT raw data and Pascal Pinter for implementing and performing orientation analysis on the aligned and cropped µCT data. The financial support of the German Research Foundation (DFG) within the project WE4273/6-1 is gratefully acknowledged.

References

[1] H.P. Degischer, F. Lasagni, M. Schöbel, T. Huber, M.A. Aly, Chapter 3: thermal expansion of Al-and Mg-Matrix composites with different reinforcement architectures, in: J.P. Davim (Ed.), Metal Matrix Composites, Nova Science Publishers, Hauppauge, N.Y, 2011, pp. 77–96.
[2] C. Zweben, Metal-matrix composites for electronic packaging, JOM 44 (7) (1992) 15–23.
[3] F. Delannay, Thermal stresses and thermal expansion in MMCs, in: A. Kelly, C.H. Zweben (Eds.), Comprehensive Composite Materials, Elsevier, Amsterdam, New York, 2000, pp. 341–369.
[4] K.U. Kainer, Grundlagen der metallmatrix-Verbundwerkstoffe, in: K.U. Kainer (Ed.), Hoboken : Metallische Verbundstoffe, John Wiley & Sons, Incorporated, 2003, pp. 1–65 Wiley-VCH [Imprint].
[5] T.W. Clyne, Thermal and conduction in MMCs, in: A. Kelly, C.H. Zweben (Eds.), Comprehensive Composite Materials, Elsevier, Amsterdam, New York, 2000, pp. 447–468.
[6] T. Huber, H.P. Degischer, G. Lefranc, T. Schmitt, Thermal expansion studies on aluminium-matrix composites with different reinforcement architecture of SiC particles, Compos. Sci. Technol. 66 (13) (2006) 2206–2217.
[7] M.H. Kural, B.K. Min, The effects of matrix plasticity on the thermal deformation of continuous fiber graphite/metal composites, J. Compos. Mater. 18 (6) (1984) 519–535.
[8] S. Kúdela, A. Rudajevová, Anisotropy of thermal expansion in Mg- and Mg4Li-matrix composites reinforced by short alumina fibers, Mater. Sci. Eng.: A 462 (1–2) (2007) 239–242.
[9] F. Lasagni, H.P. Degischer, M. Papakyriacou, Morphological changes of Si in Al-Si alloys and a short fibre composite, Kovove Materialy − Metal. Mater. 65–73 (2006) 44.
[10] X. Luo, et al., The thermal expansion behavior of unidirectional SiC fiber-reinforced Cu–matrix composites, Scr. Mater. 58 (5) (2008) 401–404.
[11] H.J. Böhm, H.P. Degischer, W. Lacom, J. Qu, Experimental and theoretical study of the thermal expansion behavior of aluminium reinforced by continuous ceramic fibers, Compos. Eng. 5 (1) (1995) 37–49.
[12] T.A. Hahn, R.W. Armstrong, Internal stress and solid solubility effects on the thermal expansivity of Al-Si eutectic alloys, Int. J. Thermophys. 9 (2) (1988) 179–193.
[13] S. Lemieux, S. Elomari, J.A. Nemes, Thermal expansion of isotropic Duralcan meta–matrix composites, J. Mater. Sci. 33 (17) (1998) 4381–4387.
[14] M. Lee, Fabrication of Ni–Nb–Ta metallic glass reinforced Al-based alloy matrix composites by infiltration casting process, Scr. Mater. 50 (11) (2004) 1367–1371.
[15] K. Lichtenberg, K.A. Weidenmann, Innovative aluminum based metallic glass particle reinforced MMCs produced by gas pressure infiltration, Mater. Sci. Forum 826 (2015) 101–108.
[16] P. Yu, et al., Fabrication and mechanical properties of Ni–Nb metallic glass particle-reinforced Al-based metal matrix composite, Scr. Mater. 54 (8) (2006) 1445–1450.
[17] Z. Wang, et al., Microstructure and mechanical behavior of metallic glass fiber-reinforced Al alloy matrix composites, (eng), Sci. Rep. 6 (2016) 24384.
[18] K. Lichtenberg, E. Orsolani-Uhlig, R. Roessler, K.A. Weidenmann, Influence of heat treatment on the properties of AlSi10Mg-based metal matrix composites reinforced with metallic glass flakes processed by gas pressure infiltration, J. Compos. Mater. 18 (2017) (002199831769986).
[19] M. Lee, D. Bae, W. Kim, D. Kim, Ni-Based refractory bulk amorphous alloys with high thermal stability, Materi. Trans. 44 (10) (2003) 2084–2087.
[20] K.K. Chawla, N. Chawla, Metal Matrix Composites, Springer Science + Business Media, Inc, Boston, MA, 2006.
[21] M. Krause, J.M. Hausherr, B. Burgeth, C. Herrmann, W. Krenkel, Determination of the fibre orientation in composites using the structure tensor and local X-ray transform, J. Mater. Sci. 45 (4) (2010) 888–896.
[22] Composight, Benjamin Bertram and Pascal Pinter, 2016.
[23] P. Pinter, S. Dietrich, K. André Weidenmann, Algorithms for the determination of orientation-tensors from three dimensional µ-CT images with various microstructures, Proceedings of the 20th International Conference on Composite Materials (2015) July.
[24] D. Kaiser, B. de Graaff, S. Dietrich, V. Schulze, A novel procedure to account for high temperature gradients in an induction dilatometer sample during rapid heating, Thermochim. Acta (2016).
[25] Bestimmung der thermischen Längenänderung fester Körper - Teil 1: Grundlagen, DIN 51045-1, 2005.
[26] S. Roy, et al., Effect of phase architecture on the thermal expansion behavior of interpenetrating metal/ceramic composites, in: N.P. Bansal (Ed.), Ceramic Transactions Series, v. 240,, Processing and Properties of Advanced Ceramics and Composites V, Wiley, Hoboken, New Jersey, 2013, pp. 33–43.
[27] M.A.M. Bourke, J.A. Goldstone, M.G. Stout, A. Needleman, Characterization of residual stresses in composites, in: S. Suresh, A. Mortensen, A. Needleman (Eds.), Fundamentals of Metal-Matrix Composites, Butterworth-Heinemann, Boston, 1993, pp. 61–80.
[28] H. Kato, H.-S. Chen, A. Inoue, Relationship between thermal expansion coefficient and glass transition temperature in metallic glasses, Scr. Mater. 58 (12) (2008) 1106–1109.
[29] Y.-Y. Wang, X.-F. Bian, R. Jia, Effects of cooling rate on thermal expansion of Cu49Hf42Al9 metallic glass, Trans. Nonferrous Met. Soc. China 21 (9) (2011) 2031–2036.
[30] M. Hansen, Constitution of Binary Alloys, 2nd ed., McGraw-Hill, New York, 1985.
[31] H.J. Axon, W. Hume-Rothery, The lattice spacings of solid solutions of different elements in aluminium, Proceedings of the Royal Society A: Mathematical, Physical and Engineering Sciences vol. 193, (1948) 1–24.
[32] R.A. Schapery, Thermal expansion coefficients of composite materials based on energy principles, J. Compos. Mater. 2 (3) (1968) 380–404.
[33] P.S. Turner, Thermal-expansion stresses in reinforced plastics, J. Res. Natl. Bur. Stan. 37 (4) (1946) 239.
[34] E.H. Kerner, The elastic and thermo-elastic properties of composite media, (en), Proc. Phys. Soc. B 69 (8) (1956) 808 http://iopscience.iop.org/article/10.1088/0370-1301/69/8/305/pdf.
[35] K. Wakashima, M. Otsuka, S. Umekawa, Thermal expansions of heterogeneous solids containing aligned ellipsoidal inclusions, J. Compos. Mater. 8 (4) (1974) 391–404.